# Dimers and chains of 3d-4f single molecule magnets constructed from heterobimetallic tectons.

Traian D. Pasatoiu, Mael Etienne, Augustin M. Madalan, Marius Andruh, Roberta Sessoli

# Dimers and chains of {3d–4f} single molecule magnets constructed from heterobimetallic tectons†

**Traian D. Pasatoiu,[a] Mael Etienne,[b] Augustin M. Madalan,[a] Marius Andruh*[a] and Roberta Sessoli*[b]**

*Received 2nd December 2009, Accepted 29th January 2010*
*First published as an Advance Article on the web 24th February 2010*
**DOI: 10.1039/b925425k**



A tetranuclear complex and a 1-D coordination polymer with a ladder-like topology have been obtained by connecting [$Ni^{II}Dy^{III}$] nodes with dicarboxylato ligands: $[Ni_2(valpn)_2Dy_2^{III}(pdca)_2(NO_3)(H_2O)_6](NO_3)\cdot 4H_2O$ **1**, and $_\infty{}^1[Ni_2(H_2O)_2(valpn)_2Dy_2(tfa)_3]\cdot 4CH_3CN$ **2** ($valpn^{2-}$ = the dianion of the Schiff base resulting from reacting *o*-vanillin with 1,3-propanediamine; $pdca^{2-}$ = the dianion of 2,6-pyridinedicarboxylic acid; $tfa^{2-}$ = the dianion of the terephthalic acid). The magnetic measurements show a ferromagnetic interaction between $Ni^{II}$ and $Dy^{III}$, and that both compounds behave like SMM with strong tunnelling. The barrier of **2** (17.4 K) is higher than that of **1** (13.6 K).

## Introduction

The synthesis of polynuclear complexes containing metal ions with Ising-type magnetic anisotropy is of great interest in molecular magnetism. Such compounds can act as nanomagnets, with a hysteresis that is observed in the absence of long-range magnetic order.[1] The nanomagnets are either clusters of various nuclearities (Single Molecule Magnets, SMMs), or one-dimensional coordination polymers (Single Chain Magnets, SCMs).[2] The combination of different spin carriers represents a powerful strategy for designing low-dimensional molecular magnets.[3] When two different metal ions are employed, at least one of them must exhibit a strong uniaxial magnetic anisotropy. Let us take the case of heterospin Single Molecule Magnets. Various combinations of spin carriers (2p-3d, 2p-4f, 3d-4f, 3d-4d, *etc.*) have been employed in order to fulfil the required conditions for the observation of SMM behavior: a high spin ground state and a large easy-axis anisotropy. The first condition is accomplished employing pairs of spin carriers that interact ferromagnetically: $Cu^{II}$–$Ln^{III}$, $Ni^{II}$–$Ln^{III}$, $rad^{\bullet}$–$Ln^{III}$.[4] The second one is fulfilled by employing strongly anisotropic metal ions: $Mn^{III}$, $Co^{II}$, $Tb^{III}$, $Dy^{III}$, $Ho^{III}$. Numerous 3d–4f SMMs have been constructed from $Cu^{II}$ and $Tb^{III}$, $Dy^{III}$, or $Ho^{III}$.[5] Other SMMs consist of high spin species obtained from nickel(II) ions interacting ferromagnetically with anisotropic lanthanides.[6] The combination of paramagnetic ligands ($rad^{\bullet}$) with lanthanides that bring magnetic anisotropy was also successful in designing SMMs.[7] Conversely, when the lanthanide is the isotropic $Gd^{III}$ ion, the second metal ion has to be anisotropic. A nice example was recently reported by Chandrasekhar, Clérac *et al.*, and contains $Gd^{III}$ and $Co^{II}$.[8] Heterometallic SMMs based on $Gd^{III}$ and $Mn^{III}$ are also known.[9] Finally, SMMs can be obtained by gathering two different anisotropic metal ions within the same molecular entity, *e.g.* $Mn^{III}$–$Ln^{III}$ ($Ln^{III}$ = $Tb^{III}$, $Dy^{III}$).[10]

The anisotropic high-spin oligonuclear complexes can be connected through various spacers resulting in 1-D coordination polymers with very interesting magnetic properties: (1) if the spacers themselves are paramagnetic, Single Chain Magnets can be obtained, the magnetic interaction between the nodes and the spacers leading to either ferromagnetic or ferrimagnetic chains;[11] (2) if the spacers are diamagnetic, chains of SMMs are formed, provided that the intermolecular interactions are weak enough to prevent the transformation of the spin network into a classical antiferromagnet.[12] Recently, Wernsdorfer *et al.*[13] and Clérac *et al.*[14] have shown that the introduction of magnetic interactions between SMMs, mediated by hydrogen bonds or bridging ligands, exerts an influence on the quantum properties, shifting the quantum tunneling resonances with respect to the isolated SMMs.

In a series of papers we have shown that large heterometallic clusters or coordination polymers can be assembled using preformed heterometallic nodes and various spacers.[15] The heterometallic nodes are easily obtained employing heterotopic compartmental ligands. Such ligands are, for example, Schiff bases derived from *o*-vanillin and diamines, originally designed by Costes to generate binuclear 3d–4f complexes.[16] Herein we report the synthesis of two 3d–4f heterometallic systems, which have been obtained following this synthetic approach: a tetranuclear complex, $[Ni_2(valpn)_2Dy_2(pdca)_2(NO_3)(H_2O)_6](NO_3)\cdot 4H_2O$ **1**, and a ladder-like coordination polymer $_\infty{}^1[Ni_2(H_2O)_2(valpn)_2Dy_2(tfa)_3]\cdot 4CH_3CN$ **2** ($H_2valpn$ is the Schiff-base resulting from the 2 : 1 condensation of 3-methoxysalicylaldehyde with propylenediamine; $pdca^{2-}$ = 2,6-pyridine-dicarboxylate; $tfa^{2-}$ = terephthalate). The binuclear node, [NiDy], has been chosen because of the magnetic anisotropy brought by the $Dy^{III}$ ion. Moreover it has

[a]*Inorganic Chemistry Laboratory, Faculty of Chemistry, University of Bucharest, Str. Dumbrava Rosie nr. 23, 020464, Bucharest, Romania. E-mail: marius.andruh@dnt.ro*
[b]*Laboratory of Molecular Magnetism, Dipartimento di Chimica e UdR INSTM di Firenze, Università degli Studi di Firenze, Polo Scientifico, Via della Lastruccia 3, 50019, Sesto Fiorentino, Firenze, Italy. E-mail: roberta.sessoli@unifi.it*

† Electronic supplementary information (ESI) available: Fig. S1, S2. CCDC reference numbers 756910 & 756911. For ESI and crystallographic data in CIF or other electronic format see DOI: 10.1039/b925425k

 

been shown that the exchange interaction between $Dy^{III}$ and $Ni^{II}$ in such compounds is ferromagnetic.[6,17]

## Experimental

### Materials

The chemicals used, *o*-vanillin, 1,3-diaminopropane, 2,6-pyridine-dicarboxylic acid, terephthalic acid, $Ni(NO_3)_2{\cdot}6H_2O$, $Dy(NO_3)_3{\cdot}5H_2O$, as well as all the solvents were purchased from commercial sources. The mononuclear complex, [Ni(valpn)], was prepared as follows: 10 mmol 1,3-propylenediamine and 20 mmol triethylamine were added under stirring to 50 mL THF solution containing 20 mmol *o*-vanillin. After 30 min, an aqueous solution (50 mL) containing 10 mmol $Ni(NO_3)_2{\cdot}6H_2O$ is added. The resulting mixture is stirred for an hour, then 500 mL $H_2O$ were added to facilitate the precipitation of the mononuclear complex. The light green solid obtained is filtered and dried. In order to synthesize the binuclear precursor, $[Ni(valpn)Dy(NO_3)(CH_3CN)(H_2O)_4]{\cdot}(NO_3)_2{\cdot}H_2O$, 4 mmol of $Dy(NO_3)_3{\cdot}5H_2O$ are added to a suspension containing 4 mmol [Ni(valpn)] in 20 mL acetonitrile. The reaction mixture is stirred for about 20 min and then left to slowly evaporate at room temperature.

**$[Ni_2(valpn)_2Dy_2(pdca)_2(NO_3)(H_2O)_6]{\cdot}4H_2O{\cdot}NO_3$ 1** was prepared as follows: three solutions, the first one containing 0.2 mmol 2,6-pyridine-dicarboxylic acid and 0.4 mmol $LiOH{\cdot}H_2O$ dissolved in 10 mL water, the second consisting of 10 mL 1 : 1 water–acetonitrile mixture, and the third one containing 0.2 mmol $[Ni(valpn)Dy(NO_3)(CH_3CN)(H_2O)_4]{\cdot}(NO_3)_2{\cdot}H_2O$ dissolved in acetonitrile were layered in a test tube. The slow diffusion of the components yielded blue crystals of the compound **1**. Calcd: 35.54 C; 3.79 H; 6.38% N. Found: 35.2 C; 3.5 H; 6.6% N.

**$_\infty{}^1[Ni_2(valpn)_2Dy_2(H_2O)_2(tfa)_3]$ 2** was prepared using a similar procedure. A solution containing 0.2 mmol terephthalic acid and 0.4 mmol $LiOH{\cdot}H_2O$ dissolved in 10 mL water, another consisting of 10 mL 1 : 1 water–acetonitrile mixture, and the third one containing 0.2 mmol $[Ni(valpn)Dy(NO_3)(CH_3CN)(H_2O)_4]{\cdot}(NO_3)_2{\cdot}H_2O$ dissolved in acetonitrile were layered in a test tube. The slow diffusion of the components yielded blue crystals of the compound **2**. Elemental chemical analyses. Calcd: 46.30 C; 3.77 H; 6.17% N. Found: 46.8 C; 3.3 H; 6.4% N.

### X-Ray structure determination

Single crystals suitable for X-ray diffraction studies were obtained by the slow diffusion technique, as described above. Data were collected at 293 K on a STOE IPDS II diffractometer using graphite-monochromated Mo-Kα radiation ($\lambda$ = 0.71073 Å). The structures were solved by direct methods and refined by full-matrix least squares techniques based on $F^2$. The non-H atoms were refined with anisotropic displacement parameters. The crystallographic data are collected in Table 1.

**Table 1** Crystallographic data, details of data collection and structure refinement parameters for compounds **1** and **2**

| Compound | **1** | **2** |
|---|---|---|
| Chemical formula | $C_{52}H_{66}N_8O_{32}Ni_2Dy_2$ | $C_{70}H_{68}N_8O_{22}Ni_2Dy_2$ |
| $M$/g mol$^{-1}$ | 1757.51 | 1815.73 |
| Temperature/K | 293(2) | 293(2) |
| Wavelength/Å | 0.71073 | 0.71073 |
| Crystal system | Monoclinic | Monoclinic |
| Space group | $P2_1/n$ | $P2_1/n$ |
| $a$/Å | 19.3054(6) | 11.6443(4) |
| $b$/Å | 15.4938(3) | 16.3722(4) |
| $c$/Å | 21.6876(7) | 19.2871(8) |
| $\alpha$ (°) | 90.00 | 90.00 |
| $\beta$ (°) | 98.176(2) | 97.641(3) |
| $\gamma$ (°) | 90.00 | 90.00 |
| $V$/Å$^3$ | 6421.1(3) | 3644.3(2) |
| $Z$ | 4 | 2 |
| $D_c$/g cm$^{-3}$ | 1.797 | 1.651 |
| $\mu$/mm$^{-1}$ | 2.975 | 2.615 |
| $F$(000) | 3432 | 1808 |
| Goodness-of-fit on $F^2$ | 1.033 | 1.114 |
| Final $R_1$, $wR_2$ [$I > 2\sigma(I)$] | 0.0507, 0.0977 | 0.0585, 0.0919 |
| $R_1$, $wR_2$ (all data) | 0.0846, 0.1068 | 0.0902, 0.0996 |
| Largest diff. peak and hole/e Å$^{-3}$ | 1.609, −1.261 | 0.844, −2.286 |

## Results and discussion

The aim of this work is to check whether our strategy for designing high-nuclearity complexes and coordination polymers, starting from heterobimetallic complexes, can be applied in order to organize SMMs into well-defined architectures. The self-assembly processes between preformed $[Ni^{II}Dy^{III}]$ complexes and the dianions of 2,6-pyridine-dicarboxylic and, respectively, terephthalic acid afford two new complexes: $[Ni_2(valpn)_2Dy_2^{III}(pdca)_2(NO_3)(H_2O)_6](NO_3){\cdot}4H_2O$ **1** and $_\infty{}^1[Ni_2(H_2O)_2(valpn)_2Dy_2(tfa)_3]{\cdot}4CH_3CN$ **2**.

### Description of the structures

The crystallographic investigation of **1** reveals cationic tetranuclear species, uncoordinated nitrate ions and water molecules. The tetranuclear species can be described as resulting from the coordination of a $\{Ni(NO_3)(H_2O)(valpn)Dy(H_2O)_2(pdca)\}$ fragment, through an oxygen atom arising from one carboxylato group, to the dysprosium ion from the second fragment, $\{Ni(H_2O)_2(valpn)Dy(H_2O)(pdca)\}$ (Fig. 1). In both fragments the nickel ions are hexacoordinated, with a slightly distorted octahedral geometry. The coordination positions around the Ni1 ion are occupied by the two nitrogen atoms [Ni1–N1 = 2.013(5); Ni1–N2 = 2.030(4) Å] and the two phenoxo oxygen atoms arising from the valpn ligand [Ni1–O2 = 2.024(3), Ni1–O3 = 2.020(3) Å], with two aqua ligands in the apical positions [Ni1–O14 = 2.107(3); Ni1–O15 = 2.121(4) Å]. The coordination sphere around the Ni2 ion is a little different. The equatorial plane is formed by the two nitrogen atoms [Ni2–N3 = 2.021(5); Ni2–N4 = 2.040(5) Å] and the two phenoxo oxygen atoms of the Schiff-base ligand [Ni2–O6 = 2.024(4), Ni2–O7 = 2.024(3) Å], and the apical positions are occupied by one aqua ligand [Ni2–O22 = 2.105(4) Å] and by one oxygen atom from a nitrato ion [Ni2–O23 = 2.160(5) Å]. Both dysprosium ions are nine-coordinated by eight oxygens and one nitrogen. The Dy1 atom is coordinated by four oxygen atoms arising from the Schiff-base [Dy1–O1 = 2.645(4); Dy1–O2 = 2.329(3); Dy1–O3 = 2.344(3); Dy1–O4 = 2.579(3) Å], one aqua ligand [Dy1–O13 = 2.408(3) Å], one nitrogen and two oxygen atoms from a $pdca^{2-}$ ligand [Dy1–O9 = 2.367(3) Å; Dy1–N7 = 2.520(4) Å; Dy1–O12 = 2.429(3) Å], as well as by a carboxylato bridging oxygen [Dy1–O16 = 2.339(3) Å]. The second dysprosium

**Table 2** Selected bond distances (Å) for $[Ni_2(valpn)_2Dy_2^{III}(pdca)_2(NO_3)(H_2O)_6](NO_3)\cdot 4H_2O$ **1**

| | | | |
|---|---|---|---|
| Ni1–N1 | 2.013(5) | Dy1–O1 | 2.645(4) |
| Ni1–N2 | 2.030(4) | Dy1–O2 | 2.329(3) |
| Ni1–O2 | 2.024(3) | Dy1–O3 | 2.344(3) |
| Ni1–O3 | 2.020(3) | Dy1–O4 | 2.579(3) |
| Ni1–O14 | 2.107(3) | Dy1–O9 | 2.367(3) |
| Ni1–O15 | 2.121(4) | Dy1–O12 | 2.429(3) |
| Ni2–N3 | 2.021(5) | Dy1–O13 | 2.408(3) |
| Ni2–N4 | 2.040(5) | Dy1–O16 | 2.339(4) |
| Ni2–O6 | 2.024(4) | Dy1–N7 | 2.520(4) |
| Ni2–O7 | 2.024(3) | Dy2–O5 | 2.579(4) |
| Ni2–O22 | 2.105(4) | Dy2–O6 | 2.303(3) |
| Ni2–O23 | 2.160(5) | Dy2–O7 | 2.307(3) |
| | | Dy2–O8 | 2.540(4) |
| | | Dy2–O17 | 2.387(4) |
| | | Dy2–O18 | 2.429(4) |
| | | Dy2–O20 | 2.435(5) |
| | | Dy2–O21 | 2.438(5) |
| | | Dy2–N8 | 2.500(4) |

atom, Dy2, is coordinated by the four oxygen atoms of the Schiff base [Dy2–O5 = 2.579(4); Dy2–O6 = 2.303(3); Dy2–O7 = 2.307(3); Dy2–O8 = 2.540(4) Å], two aqua ligands [Dy2–O20 = 2.435(5) Å; Dy2–O21 = 2.438(5) Å] and three donor atoms from a 2,6-pyridine-dicarboxylato ligand [Dy2–O17 = 2.387(4); Dy2–N8 = 2.500(4); Dy2–O18 = 2.429(4) Å]. The Ni···Dy distances are around 3.5 Å (Ni1···Dy1 = 3.498; Ni2···Dy2 = 3.464 Å), while the two Dy ions are placed approximately twice as far (Dy1···Dy2 = 6.788 Å). Selected bond distances are collected in Table 2.

Compound **2** is a 1-D coordination polymer with a ladder-like topology (Fig. 2). A step of the ladder is made by a $[Ni_2(H_2O)_2(valpn)_2Dy_2(tfa)]^{2+}$ moiety, which results by connecting two $[Ni(valpn)Dy(H_2O)]^{3+}$ nodes by a terephthalato spacer. The neighbouring steps of the ladder are connected through other terephthalato anions, two for each $[Ni_2(H_2O)_2(valpn)_2Dy_2(tfa)]^{2+}$ unit. Two types of terephthalato spacers are observed within the structure of compound **2**. The first type is a symmetrical one, the terephthalato anion connecting

**Table 3** Selected bond distances (Å) for $_\infty{}^1[Ni_2(H_2O)_2(valpn)_2Dy_2(tfa)_3]\cdot 4CH_3CN$ **2**

| | | | |
|---|---|---|---|
| Ni1–N1 | 2.026(4) | Dy1–O1 | 2.644(3) |
| Ni1–N2 | 2.048(4) | Dy1–O2 | 2.282(3) |
| Ni1–O2 | 2.038(3) | Dy1–O3 | 2.295(3) |
| Ni1–O3 | 2.007(3) | Dy1–O4 | 2.532(3) |
| Ni1–O8 | 2.038(3) | Dy1–O5 | 2.427(3) |
| Ni1–O11 | 2.203(3) | Dy1–O6 | 2.493(3) |
| | | Dy1–O7 | 2.381(3) |
| | | Dy1–O9 | 2.427(3) |
| | | Dy1–O10 | 2.438(3) |

two dysprosium ions from two heterodinuclear nodes within one step of the ladder, and each carboxylato group chelates a dysprosium ion. The second coordination mode consists of an asymmetrical bridge formed between two adjacent ladder steps: one carboxylato group is chelating a dysprosium ion, while the second one coordinates to the dysprosium and nickel ions from a binuclear node.

The nickel ions display a slightly elongated octahedral geometry, with the equatorial positions occupied by two nitrogen atoms and two phenoxo oxygen atoms of the Schiff-base ligand [Ni1–O2 = 2.038(3), Ni1–O3 = 2.007(3), Ni1–N1 = 2.026(4), Ni1–N2 = 2.048(4) Å], while the axial positions are filled by one aqua ligand [Ni1–O11 = 2.203(3) Å], and one oxygen atom from a bridging carboxylato group [Ni1–O8 = 2.038(3) Å]. The dysprosium ions are surrounded by nine oxygen atoms: four oxygen atoms arise from the $valpn^{2-}$ ligand [Dy1–O1 = 2.644(3) Å; Dy1–O2 = 2.282(3) Å; Dy1–O3 = 2.295(3) Å; Dy1–O4 = 2.532(3) Å] and five others form three terephthalato spacers, *i.e.* two chelating carboxylato groups and one carboxylato group that bridges one nickel and one dysprosium ion [Dy1–O5 = 2.427(3) Å; Dy1–O6 = 2.493(3) Å; Dy1–O7 = 2.381(3) Å; Dy1–O9 = 2.427(3) Å; Dy1–O10 = 2.438(3) Å]. The Ni···Dy distance within a node is 3.383 Å, while the shortest internode Dy···Dy distances are Dy···Dy″ = 11.334 Å and Dy···Dy′ = 11.643 Å. Selected bond distances are gathered in Table 3.

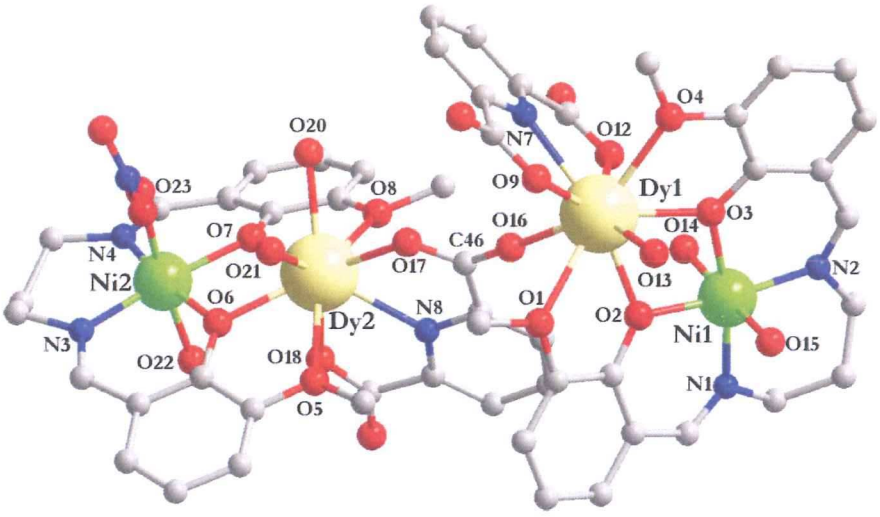


**Fig. 1** Perspective view of the tetranuclear complex **1**, along with the atom numbering scheme.

 

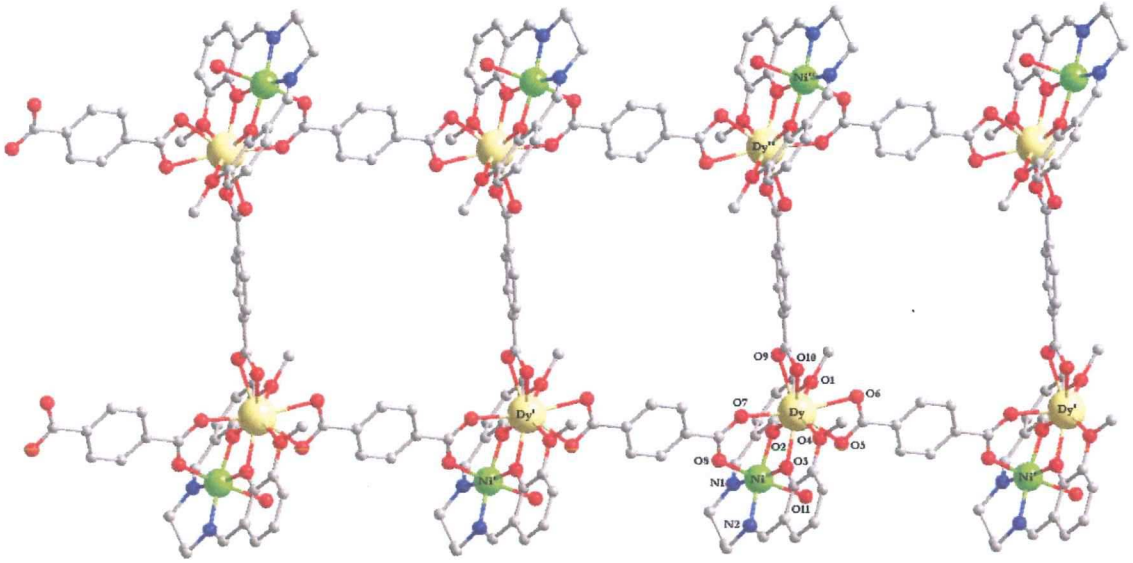


**Fig. 2** Perspective view of the ladder-like coordination polymer **2**, and labeling scheme (□□ = −1 + *x*, *y*, *z*; □ = 2 − *x*, 1 − *y*, − *z*).

### Magnetic properties

The static and dynamic magnetic properties of compounds **1** and **2** have been investigated. Let us start with the tetranuclear compound, **1**. The temperature variation of the $\chi_M T$ product per tetranuclear unit is represented in Fig. 3. At room temperature the value of $\chi_M T$ is 29.94 emu mol$^{-1}$ K, which corresponds well to the four uncoupled paramagnetic centers: two Ni$^{II}$ ions ($S = 1$, $g = 2$) and two Dy$^{III}$ ions ($J = 15/2$, $S = 5/2$, $L = 5$, $^6H_{15/2}$, $g_{15/2} = 4/3$), the expected value being 30.34 emu mol$^{-1}$ K. By lowering the temperature, $\chi_M T$ decreases continuously down to 12 K due to the depopulation of the Stark levels of the Dy$^{III}$ ions. Below this temperature it remains almost flat, only slightly increasing, then to decrease below 6 K, reaching 24.96 emu mol$^{-1}$ K at 2 K. The field dependence of the magnetization has been measured at $T = 2$ K and the results are reported in Fig. 4. The magnetization rapidly increases up to 10 kOe to reach *ca.* 11 $\mu_B$ with a weak but linear increase for higher field.

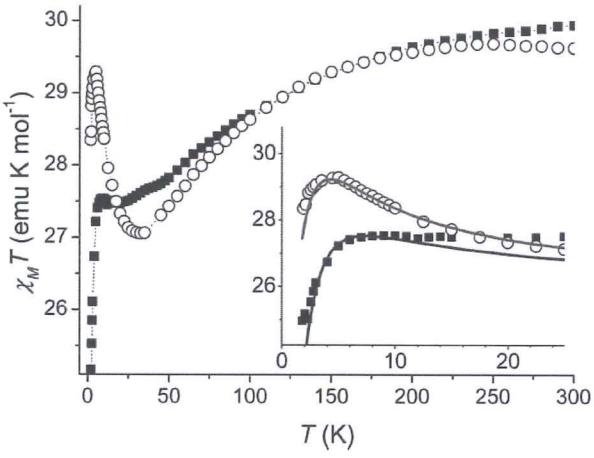


**Fig. 3** Plot of $\chi_M T$ *versus* $T$ curves recorded for compound **1** (solid squares) and for **2** (open circles). In the inset the low temperature region is enlarged and the calculated $\chi_M T$ values are reported as solid grey lines (see text for the parameters).

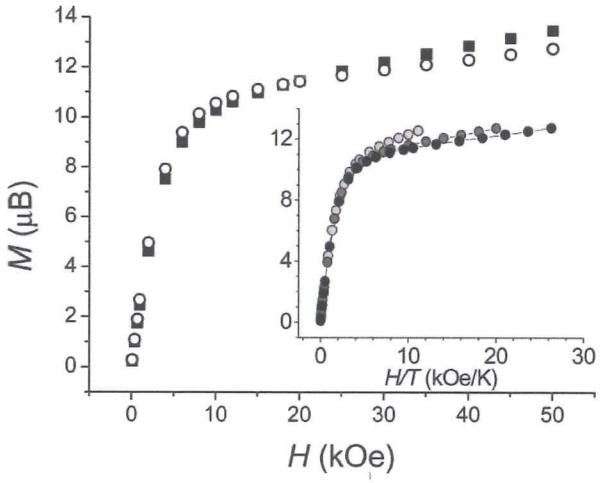


**Fig. 4** Field dependence of the magnetization for **1** (solid squares) and for **2** (open circles) measured at $T = 2$ K. In the inset the data for **2** measured at $T = 1.8$ K (black), 2.4 K (dark grey) and 4.4 K (grey) are plotted *vs.* the scaled variable $H/T$ to evidence deviations from superposition at high fields.

A slightly different $\chi_M T$ behaviour has been observed for **2**, as shown in Fig. 3. The typical decrease of the $\chi_M T$ starts around 250 K but a more evident upturn is observed below 30 K, with $\chi_M T$ going from 27.06 to 29.29 emu K mol$^{-1}$. Also in this case a decrease is observed below 5 K. The magnetization *versus* field curve is very similar to that of **1**, showing however a weaker increase at high field. The temperature dependence of the magnetization is very typical of anisotropic materials, and rescaling the data by plotting $M$. *vs* $H/T$ gives superimposable curves only for lower fields (see inset of Fig. 4).

In order to get some qualitative information on the magnetic exchange involving the dysprosium and nickel pairs we have tried to simulate the low temperature behaviour assuming for the Dy(III) ions an effective spin $S_{eff} = 1/2$ with Ising type anisotropy.[18] We have first analyzed the behaviour of **2** by assuming that the exchange interactions mediated by the $tfa^{2-}$ ligands are negligible, thus reducing the Spin Hamiltonian to:

$$H_{pair} = -J^{z}_{Dy-Ni} S^{z}_{Ni} S^{z}_{Dy} + D_{Ni}[S^{z}_{Ni}{}^{2} - 1/3 S_{Ni}(S_{Ni} + 1)] + g^{z}_{Dy} \mu_B H^{z} S^{z}_{Dy} + g_{Ni} \mu_B \mathbf{H} \cdot \mathbf{S}_{Ni} \quad (1)$$

The data in the inset of Fig. 3 are satisfactorily reproduced assuming $g^{z}_{Dy} = 19.4$, $g^{x,y}_{Dy} = 1$, $g_{Ni} = 2.2$, $D_{Ni} = 4$ cm$^{-1}$, and $J^{z}_{Ni-Dy} = 6$ cm$^{-1}$. The large value estimated for $g^{z}_{Dy}$ is typical of this ion and confirms the validity of the Ising model we have employed.[18a,19] The increase of $\chi_M T$ below 30 K is therefore attributed to the ferromagnetic exchange interaction between Ni–Dy, in agreement with what is observed in phenoxo-bridged Ni–Gd pairs.[6d,17] The exchange energy however appears smaller for $Dy^{III}$ than for $Gd^{III}$ despite the larger $J$ value, as here an $S_{eff} = 1/2$ is employed. No magneto-structural correlations are available for Dy–M pairs as in most cases the analysis of the magnetic data is only performed at a qualitative level. The decrease of $\chi_M T$ below 5 K is well accounted for by the single ion anisotropy of $Ni^{II}$, therefore hampering any estimation of the interactions mediated by the terephthalate ligand.

The Spin Hamiltonian parameters obtained for **2** have been employed for **1**, where we have added the Dy–Dy interaction mediated by the carboxylato bridge. The Spin Hamiltonian becomes:

$$H_{tetra} = H^{A}_{pair} + H^{B}_{pair} - J^{z}_{Dy-Dy} S^{z}_{Dy\,A} S^{z}_{Dy\,B} \quad (2)$$

where A and B refer to the two Ni–Dy pairs here assumed identical despite the significant structural differences. The very low temperature decrease is well reproduced by adding an antiferromagnetic Dy···Dy interaction $J^{z}_{Dy-Dy} = -1$ cm$^{-1}$. According to literature data,[20] the exchange interaction between 4f metal ions bridged by the carboxylato group is supposed to be very weak. This value is however just indicative, as the single ion anisotropy of the Ni ion can be different from that estimated in **2**. Moreover, dipolar interactions are of the same order of magnitude but hard to estimate without a precise knowledge of the orientation of the easy axes of the Dy ions.[19c] It must be noticed that the experimental $\chi_M T$ continues to decrease down to *ca.* 12 K in **1**. As a constant $\chi_M T$ would imply that only the ground doublet is populated we deduce that the first excited doublet of the $J = 15/2$ multiplet is much closer in energy for **1** than for **2**. This is in agreement with the higher slope in the $M$ *vs.* $H$ curve at high fields observed for **1**. The assumption of our simplified Ising Spin Hamiltonian seems therefore less appropriate for this system than for **2**. Moreover, in the absence of additional information from single crystal data all anisotropy axes have been assumed to be collinear. Non-collinearity of easy axes in molecular systems comprising $Dy^{III}$ has been recently shown to affect substantially the magnetic behaviour.[21]

The dynamic magnetic behavior of **1** was investigated in the 0.2–25 kHz range by using alternating current (ac) susceptometry. In zero static field both in-phase ($\chi'$) and out-of-phase ($\chi''$) components of the magnetic susceptibility show frequency dependence (Fig. 5). The shape of the signals is broad, without maxima, suggesting multiple relaxation processes, as well as fast quantum tunneling of the magnetization. This effect is even more evident in the zero field ac data of **2**, which reveal the typical levelling of $\chi''$ (Fig. 6). Peaks in $\chi''$ *vs.* $T$ are observed when the variation of the relaxation time, $\tau$, with temperature allows them to go through the condition for maximum $\chi''$ signal, *i.e.* $\omega\tau = 1$ with $\omega$ the angular frequency of the ac field. When the relaxation time depends weakly on temperature, *i.e.* in the presence of tunneling, these peaks become severely distorted and an accurate estimation of the relaxation time can only be done by plotting $\chi''$ as a function of the frequency of the oscillating field as done in Fig. 7. While **1** does not show maxima, these are well defined for **2** but they become almost temperature independent below 2 K. The tunneling rate is therefore estimated to be of the order of 2 kHz, while the extracted relaxation times are reported in the Arrhenius plot of Fig. 8. The data strongly deviate from a linear behaviour with the relaxation time approaching saturation at low temperature. By only fitting the high temperature data and assuming $\tau = \tau_0 \exp(\Delta/kT)$ a very small energy barrier $\Delta = 2$ K is estimated, associated to a very large pre-exponential factor $\tau_0 = 1.3 \times 10^{-5}$ s, confirming that we are observing a smooth transition between a thermally activated regime and a quantum tunneling one.

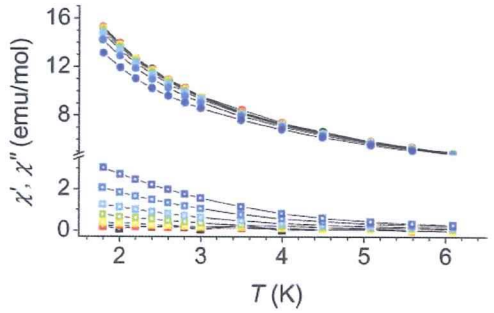


**Fig. 5** Real (solid circles) and imaginary (open squares) components of the ac susceptibility of **1** measured in zero static field and in the frequency range 0.2–25 kHz (colour scale from red to blue).

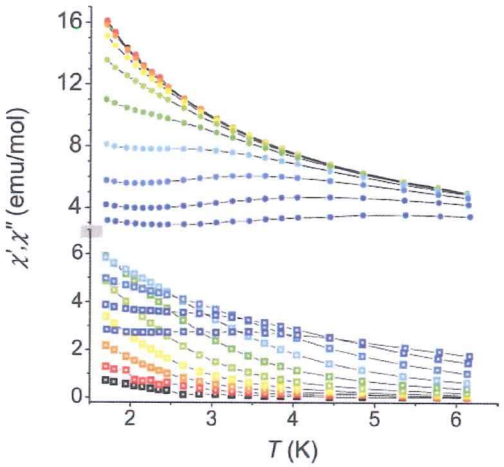


**Fig. 6** Real (solid circles) and imaginary (open squares) components of the ac susceptibility of **2** measured in zero static field and in the frequency range 0.2–25 kHz (colour scale from red to blue).

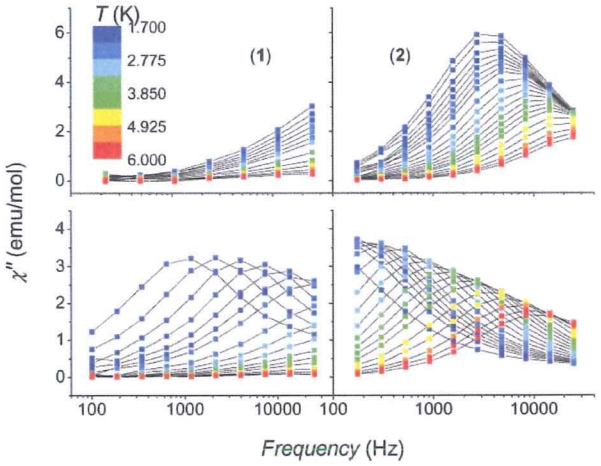


**Fig. 7** Frequency dependence of the imaginary components of the ac susceptibility of **1** (left) and of **2** (right) measured in zero static field upper panels and in a static magnetic field of 750 and 1000 Oe for **1** and **2**, respectively (lower panels). Temperature color scheme in the legend.

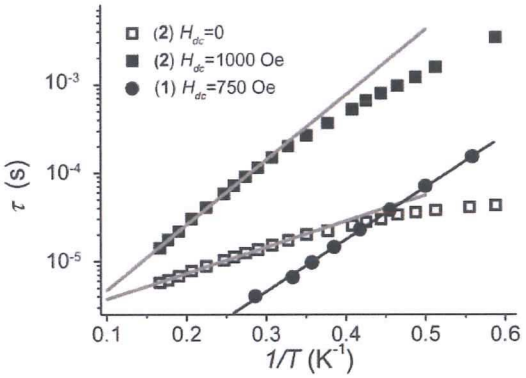


**Fig. 8** Temperature dependence of the relaxation time reported as an Arrhenius plot for **1** in 750 Oe static field and for **2** in both zero and 1000 Oe static field. The solid lines represent the linear fit as described in the text.

The analysis of the magnetization dynamics in lanthanide-based SMMs is much more complex than in the case of metal ions with quenched orbital momentum, for which the Spin Hamiltonian approach is able to rationalize most observations.[2] It is generally assumed that relaxation at intermediate temperatures, *i.e.* lower then the Debye temperature of the system, occurs through a thermally activated process that involves the first excited Stark levels.[22] However, especially for low symmetric environments, the transverse components of the crystal fields efficiently admix the states on opposite sides of the barrier generated by the Ising anisotropy. It is thus rather common to observe below 4 K an efficient underbarrier mechanism of relaxation.[4b,7] This is indeed what is observed in **1** and **2**.

The mechanism of quantum tunneling can be reduced by applying a static field that removes the degeneracy of the levels on the opposite sides of the barrier.[2] For this reason the ac measurements were also carried out in the presence of a static field, which was selected to be 750 Oe and 1000 Oe for **1** and **2**, respectively, by scanning the field at $T = 2$ K and selecting the one that shifts the peak in $\chi''$ to the lowest frequency. $\chi''$ now exhibits a frequency maxima for both compounds (lower part of Fig. 7), allowing an estimation of the Arrhenius parameters also for **1**, *i.e.* $\Delta = 13.6$ K and $\tau_0 = 7.7 \times 10^{-8}$ s, the last value being typical of SMM behaviour. The same analysis performed on **2** provides $\Delta = 17.4$ K and $\tau_0 = 8.0 \times 10^{-7}$ s. These parameters are extracted from the high temperature data to exclude from the fitting the curvature observed at low temperature but are anyhow only indicative of the energy gap between the ground and the first excited doublets. Interestingly a smaller $\Delta$ value is observed for **1**, in agreement with the trend observed for both $\chi_M T$ *vs.* $T$ and $M$ *vs.* $H$ curves. The application of a static field, despite its strong effect, does not seem to be able to totally suppress tunnelling in **2**, in contrast with that observed in **1**. This is not surprising, because in **2** tunneling has shown to be very efficient.

Another important parameter is the width of the distribution of the relaxation time, which has been investigated by plotting $\chi''$ *vs.* $\chi'$ in the so called Argand plot (see Fig. S1 and S2 in ESI†). The deviations from the ideal behaviour of a single relaxation time that results in a semicircle are taken into account by an empirical parameter $\alpha$.[23] For **1** this parameter has been found to oscillate between 0.16 and 0.24, without any distinct trend. Such values are rather common in SMM.[2,24]

In the case of **2** a constant increase from $\alpha = 0.10$ to 0.30 on decreasing the temperature is observed. This trend is usually encountered when at low temperature, quantum tunnelling becomes efficient,[24c-e] and suggests that disorder or defects more strongly affect the admixing of the states, and thus the tunneling rate, than the height of the barrier.

## Conclusions

The new systems described here illustrate that anisotropic high spin 3d–4f binuclear complexes can be organized in either high-nuclearity clusters or in coordination polymers, preserving their SMM behavior. Both compounds exhibit a strong tunnelling, despite the chain character of **2**. This is not surprising as we have no evidence of a sizeable interaction mediated by the $tfa^{2-}$ diamagnetic ligands. On the other hand, as shown in a previous paper,[11] a chain of SMMs can be transformed into a SCM by connecting the heterometallic nodes through paramagnetic spacers, *e. g.* metalloligands. The barrier observed for **2** is however higher than that of **1**, in agreement with the static properties that suggests a larger separation between the ground and the first excited doublet of the $Dy^{III}$ Stark levels. Surprisingly, tunnelling also survives in a static field for **2**, while it is more efficiently suppressed in **1**. We can tentatively attribute this observation to the weak Dy–Dy interaction present in **1** in analogy with that observed in a Dy-Radical tetramer.[7] Further investigations performed for instance by diluting the Dy–Ni pairs in diamagnetic analogues containing yttrium are necessary to confirm this hypothesis.

## Acknowledgements

This work was financially supported by the CNCSIS (PNII–IDEI-1912/2009) and by the EC through NoE MAGMANet (NMP3-CT-2005-515767). M. E. acknowledges the EC (MCTS-Molmag-NEST-CT-2004-504204) and the German DFG (SPP-1137 Molekularer Magnetismus) for doctoral grants.

## References


1 R. Sessoli, D. Gatteschi, A. Caneschi and M. A. Novak, *Nature*, 1993, **365**, 141.

2 (*a*) D. Gatteschi, R. Sessoli and J. Villain, *Molecular Nanomagnets*, Oxford University Press, 2006; (*b*) D. Gatteschi and R. Sessoli, *Angew. Chem., Int. Ed.*, 2003, **42**, 268.

3 (*a*) G. Aromi and E. K. Brechin, *Struct. Bonding*, 2006, **122**, 1; (*b*) C. Coulon, H. Miyasaka and R. Clérac, *Struct. Bonding*, 2006, **122**, 163; E. K. Brechin, *Chem. Commun.*, 2005, 5141; J. N. Rebilly and T. Mallah, *Struct. Bonding*, 2006, **122**, 103; (*c*) L. Bogani, A. Vindigni, R. Sessoli and D. Gatteschi, *J. Mater. Chem.*, 2008, **18**, 4750.

4 Recent reviews: (*a*) M. Andruh;, J.-P. Costes, C. Diaz and S. Gao, *Inorg. Chem.*, 2009, **48**, 3342; (*b*) R. Sessoli and A. K. Powell, *Coord. Chem. Rev.*, 2009, **253**, 2328.

5 See, for example: (*a*) J. P. Costes, F. Dahan and W. Wernsdorfer, *Inorg. Chem.*, 2006, **45**, 5; (*b*) C. Aronica, G. Pilet, G. Chastanet, W. Wernsdorfer, J. F. Jacquot and D. Luneau, *Angew. Chem., Int. Ed.*, 2006, **45**, 4659; (*c*) J.-P. Costes, M. Auchel, F. Dahan, V. Peyron, S. Shova and W. Wernsdorfer, *Inorg. Chem.*, 2006, **45**, 1924; (*d*) T. Hamamatsu, K. Yabe, M. Towatari, S. Osa, N. Matsumoto, N. Re, A. Pochaba, J. Mrozinski, J.-L. Gallani, A. Barla, P. Imperia, C. Paulsen and J.-P. Kappler, *Inorg. Chem.*, 2007, **46**, 4458; (*e*) T. Kajiwara, M. Nakano, S. Takaishi and M. Yamashita, *Inorg. Chem.*, 2008, **47**, 8604; (*f*) G. Novitchi, W. Wernsdorfer, L. F. Chibotaru, J.-P. Costes, C. E. Anson and A. K. Powell, *Angew. Chem., Int. Ed.*, 2009, **48**, 1614.

6 (*a*) F. Pointillart, K. Bernot, R. Sessoli and D. Gatteschi, *Chem.–Eur. J.*, 2007, **13**, 1602; (*b*) V. Chandrasekhar, B. M. Pandian, R. Boomishankar, A. Steiner, J. J. Vittal, A. Houri and R. Clérac, *Inorg. Chem.*, 2008, **47**, 4918; (*c*) F. Mori, T. Ishida and T. Nogami, *Polyhedron*, 2005, **24**, 2588; (*d*) T. Yamaguchi, Y. Sunatsuki, H. Ishida, M. Kojima, H. Akashi, N. Re, N. Matsumoto, A. Pochaba and J. Mrozinski, *Inorg. Chem.*, 2008, **47**, 5736.

7 G. Poneti, K. Bernot, L. Bogani, A. Caneschi, R. Sessoli, W. Wernsdorfer and D. Gatteschi, *Chem. Commun.*, 2007, 1807.

8 V. Chandrasekhar, B. M. Pandian, R. Azhakar, J. J. Vittal and R. Clérac, *Inorg. Chem.*, 2007, **46**, 5140.

9 (*a*) V. Mereacre, A. M. Ako, R. Clérac, W. Wernsdorfer, I. J. Hewitt, C. E. Anson and A. K. Powell, *Chem.–Eur. J.*, 2008, **14**, 3577; (*b*) T. C. Stamatos, S. J. Teat, W. Wernsdorfer and G. Christou, *Angew. Chem., Int. Ed.*, 2009, **48**, 521.

10 C. M. Zaleski, E. C. Depperman, J. W. Kampf, M. L. Kirk and V. L. Pecoraro, *Angew. Chem., Int. Ed.*, 2004, **43**, 3912.

11 D. Visinescu, A. M. Madalan, M. Andruh, C. Duhayon, J.-P. Sutter, L. Ungur, W. Van den Heuvel and L. F. Chibotaru, *Chem.–Eur. J.*, 2009, **15**, 11808.

12 R. Inglis, L. F. Jones, K. Mason, A. Collins, S. A. Moggach, S. Parson, S. P. Perlepes, W. Wernsdorfer and E. K. Brechin, *Chem.–Eur. J.*, 2008, **14**, 9117.

13 W. Wernsdorfer, N. Aliaga-Alcalde, D. N. Hendrickson and G. Christou, *Nature*, 2002, **416**, 406.

14 (*a*) L. Lecren, O. Roubeau, Y.-G. Li, X. F. Le Goff, H. Miyasaka, F. Richard, W. Wernsdorfer, C. Coulon and R. Clérac, *Dalton Trans.*, 2008, 755; (*b*) O. Roubeau and R. Clérac, *Eur. J. Inorg. Chem.*, 2008, 4315; (*c*) L. Lecren, W. Wernsdorfer, Y.-G. Li, A. Vindigni, H. Miyasaka and R. Clérac, *J. Am. Chem. Soc.*, 2007, **129**, 5045.

15 (*a*) M. Andruh, *Pure Appl. Chem.*, 2005, **77**, 1685; (*b*) M. Andruh, *Chem. Commun.*, 2007, 2565; (*c*) R. Gheorghe, P. Cucos, M. Andruh, J. P. Costes, B. Donnadieu and S. Shova, *Chem.–Eur. J.*, 2006, **12**, 187; (*d*) M. Andruh, D. G. Branzea, R. Gheorghe and A. M. Madalan, *CrystEngComm*, 2009, **11**, 2571.

16 J.-P. Costes, F. Dahan, A. Dupuis and J.-P. Laurent, *Inorg. Chem.*, 1996, **35**, 2400.

17 (*a*) T. Shiga, N. Ito, A. Hidaka, H. Ohkawa, S. Kitagawa and M. Ohba, *Inorg. Chem.*, 2007, **46**, 3492; (*b*) C. A. Barta, S. R. Bayly, P. W. Read, B. O. Patrick, R. C. Thompson and C. Orvig, *Inorg. Chem.*, 2008, **47**, 2280; (*c*) S. Dhers, S. Sahoo, J.-P. Costes, C. Duhayon, S. Ramasesha and J.-P. Costes, *CrystEngComm*, 2009, **11**, 2078; (*d*) J.-P. Sutter, S. Dhers, R. Rajamani, S. Ramasesha, J.-P. Costes, C. Duhayon and L. Vendier, *Inorg. Chem.*, 2009, **48**, 5820; (*e*) J.-P. Costes, T. Yamaguchi, M. Kojima and L. Vendier, *Inorg. Chem.*, 2009, **48**, 5555; (*f*) J.-P. Costes, F. Dahan, A. Dupuis and J.-P. Laurent, *Inorg. Chem.*, 1997, **36**, 4284.

18 (*a*) R. D. L. Carlin, *Magnetochemistry*, Springer-Verlag, Berlin, 1986; (*b*) W. P. Wolf, *Braz. J. Phys.*, 2000, **30**, 794.

19 (*a*) L. F. Chibotaru, L. Ungur and A. Soncini, *Angew. Chem., Int. Ed.*, 2008, **47**, 4126; (*b*) K. Bernot, J. Luzon, L. Bogani, M. Etienne, C. Sangregorio, M. Shanmugam, A. Caneschi, R. Sessoli and D. Gatteschi, *J. Am. Chem. Soc.*, 2009, **131**, 5573; (*c*) I. J. Hewitt, Y. Lan, C. E. Anson, J. Luzon, R. Sessoli and A. K. Powell, *Chem. Commun.*, 2009, 6765.

20 See, for example: (*a*) L. Canadillas-Delgado, J. Pasán, O. Fabelo, M. Hernández-Molina, F. Lloret, M. Julve and C. Ruiz-Pérez, *Inorg. Chem.*, 2006, **45**, 10585, and references therein.

21 (*a*) J. Luzon, K. Bernot, I. J. Hewitt, C. E. Anson, A. K. Powell and R. Sessoli, *Phys. Rev. Lett.*, 2008, **100**, 247205; (*b*) K. Bernot, J. Luzon, R. Sessoli, A. Vindigni, J. Thion, S. Richeter, D. Leclercq, J. Larionova and A. Van Der Lee, *J. Am. Chem. Soc.*, 2008, **130**, 1619.

22 (*a*) A. Abragam and B. Bleaney, *Electron Paramagnetic Resonance of Transition Ions*, Dover, New York, 1986; (*b*) N. Ishikawa, *Polyhedron*, 2007, **26**, 2147.

23 K. S. Cole and R. H. Cole, *J. Chem. Phys.*, 1941, **9**, 341.

24 (*a*) M.-H. Zeng, M.-X. Yao, H. Liang, W.-X. Zhang and X.-M. Chen, *Angew. Chem., Int. Ed.*, 2007, **46**, 1832; (*b*) D. Wu, D. Guo, Y. Song, W. Huang, C.-Y. Duan, Q.-J. Meng and O. Sato, *Inorg. Chem.*, 2009, **48**, 854; (*c*) A. Cornia, L. Gregoli, C. Danieli, A. Caneschi, R. Sessoli, L. Sorace, A. L. Barra and W. Wernsdorfer, *Inorg. Chim. Acta*, 2008, **361**, 3481; (*d*) L. Gregoli, C. Danieli, A. L. Barra, P. Neugebauer, G. Pellegrino, G. Poneti, R. Sessoli and A. Cornia, *Chem.–Eur. J.*, 2009, **15**, 6456; (*e*) T. Kajiwara, K. Takahashi, T. Hiraizumi, S. Takaishi and M. Yamashita, *Polyhedron*, 2009, **28**, 1860.


 